Design of Implantable Rectangular Spiral Antenna for Wireless Biotelemetry in MICS Band

Jae-Ho Lee, Dong-Wook Seo, and Hyung Soo Lee

For this study, we designed an implantable rectangular spiral antenna for medical biotelemetry in the Medical Implant Communications Service band (402 MHz to 405 MHz). The designed antenna has a U-shaped loop for impedance matching. The antenna impedance is easily adjusted by controlling the shape and length of the U-shaped loop. Significant design parameters were studied to understand their effects on the antenna performance. To verify the potential of the antenna for the desired applications, we fabricated a prototype and measured its performance in terms of the resonant characteristics and gain radiation patterns of the antenna. In the testing phase, the prototype antenna was embedded in human skin tissue–emulating gel, which was developed to simulate a real operation environment. The measured resonant characteristics show good agreement with the simulations, and the –10 dB frequency band is within the range of 398 MHz to 420 MHz. The antenna exhibits a maximum gain of –22.26 dBi and an antenna efficiency of 0.215%.

Keywords: Implantable antenna, rectangular spiral antenna, wireless biotelemetry, Medical Implant Communications Service, MICS.

Manuscript received May 2, 2014; revised July 17, 2014; accepted July 31, 2014.

This work was supported by the MSIP (the Ministry of Science, ICT, and Future Planning), Rep. of Korea (No. 10041876).

Jae-Ho Lee (jhlee1229@etri.re.kr), Dong-Wook Seo (corresponding author, seodongwook@etri.re.kr), and Hyung Soo Lee (hsulee@etri.re.kr) are with the IT Convergence Technology Research Laboratory, ETRI, Daegu, Rep. of Korea.

I. Introduction

Nowadays, wireless technologies for various medical applications have attracted a lot of interest with the growing need to improve patient comfort and care [1]–[5]. In particular, one of the latest developments is in the field of wireless medical telemetry between implanted devices and external equipment for diagnostic and monitoring purposes [6]. For wireless communication with medical implants, several frequency bands have been allocated; however, the most commonly used band is the Medical Implant Communications Service (MICS) frequency band (402 MHz to 405 MHz) assigned by the Federal Communications Commission [7]. MICS has replaced the previous low-frequency inductive link with radio-frequency linked communication; the latter can overcome the drawbacks of the former, such as a slow data rate, short-range communication, and sensitivity to the positioning between the inner and outer coils [8]–[9].

Implanted devices are inserted into a human or animal body and communicate physiological information, such as glucose level, blood pressure, and temperature, to external equipment. An implantable antenna ensures wireless biotelemetry and is, therefore, a crucial part of the implanted components, which also include a transceiver, chips with circuits, and biosensors. The fact that an implantable antenna has to work inside the human body makes the antenna design very challenging. In general, design of an implantable antenna should take into account miniaturization, biocompatibility, impedance matching, far-field gain, and patient safety, among other aspects [10].

A variety of implantable antennas have been investigated for use in biotelemetry. A patch design has received wide attention for such application thanks to its well-known flexibility in shape, conformability, and miniaturization [11]–

[12]. To emphasize the miniaturization, circular- and square-shaped planar-inverted F-antennas with a stacked structure have been suggested for biotelemetry in the MICS band [13]–[14]. For the same application, meandering- and spiral-shaped patches have also been presented [15]–[20].

For this study, we consider an implantable rectangular spiral-shaped configuration and evaluate the potential of the antenna for use in biotelemetry within the MICS band. To reduce the size of the antenna, a spiraling of the conductor patch was realized on a high-permittivity dielectric substrate material. The antenna has a U-shaped loop structure to transform the antenna impedance to the desired value [21]. The antenna impedance can be easily adjusted by controlling the shape and length of the U-shaped loop. Several parameters were studied to obtain a complete insight into the antenna performance. Simulations and designs were carried out based on Ansoft's EM simulator, HFSS. To account for a general tissue implantable antenna, a single-layer-of-human-skin-tissue-model is assumed [10]. The potential of the antenna design was verified through manufacturing a prototype and measuring its resonance characteristics and gain radiation patterns in the MICS band. To provide a real operation environment for the antenna, we developed a human skin tissue–emulating material that had similar electrical properties to those of human skin (ε_r = 46.7 and σ = 0.69 S/m at 402 MHz) [22].

II. Antenna Geometry

The configuration of the considered rectangular spiral antenna and its geometric parameters are shown in Fig. 1. A conducting spiral configuration with a U-shaped loop structure of 0.5 mm in width and 18 μm in thickness was printed on a 0.635 mm thick (t_1) high-permittivity dielectric substrate (ε_r = 10.2, tan δ = 0.03) and covered with a bio-compatible superstrate layer (ε_r = 3.78). Since human tissue is lossy and conductive, the superstrate layer plays a role in preventing an undesirable short-circuit by separating the metallic radiator from the human tissue. A 1 mm thick (t_2) superstrate was considered for this study. Consequently, the size of the antenna is 20 mm × 10 mm × 1.653 mm, which is quite pertinent to an implanted wireless system. The width and spacing between the edges of the spiral-shaped conductors are set to 0.5 mm and 0.4 mm, respectively, to simplify the design parameters. A U-shaped loop structure with u_1 = 1.6 mm is used to match the antenna impedance to 50 Ω feeding.

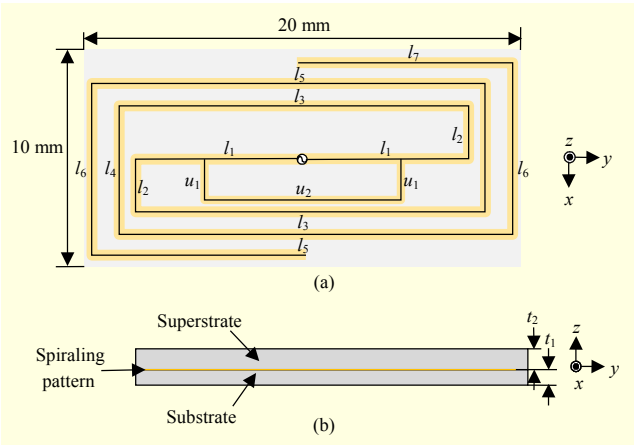

Fig. 1. Geometry of designed antenna: (a) top view and (b) side view.

III. Antenna Design and Parametric Studies

1. Antenna Design and Simulation Results

A. Antenna Design

The simulation model for the antenna design is presented in Fig. 2. The antenna was placed inside of a 100 mm × 100 mm × 20 mm simplified canonical human skin tissue model (ε_r = 46.7 and σ = 0.69 S/m at 402 MHz) to take account of the operating environment, and it was located at a depth of 10 mm under the skin. The antenna simulation was conducted using the HFSS.

A three-step process was used for an efficient design. In the first step, since the spiral can be thought of as a modified dipole, an initial total spiral length of about half a wavelength (58.7 mm) was adopted without a U-shaped loop and then manually modified to resonate at the design frequency (403.5 MHz). In the next step, the U-shaped loop is attached to the spiral configuration, as shown in Fig. 1. The small spiral configuration has impedance with a small radiation resistance and capacitive reactance; hence, the attached U-shaped loop provides the antenna with an impedance transformation, increasing both the resistance and the shunt inductance, which cancels the capacitive part of the antenna impedance and achieves a matching with the feeding impedance. In the final step, the spiral lengths (l_1 through l_7) and U-shaped loop length (u_2) are simultaneously modified until the antenna resonates at the desired frequency. The resonance frequency and antenna

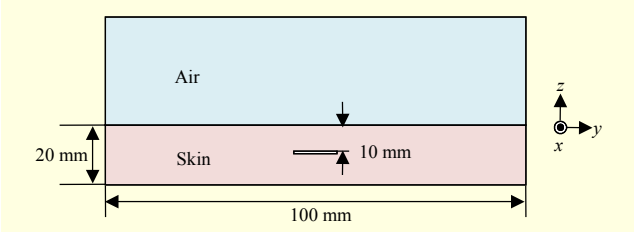

Fig. 2. Simulation model for antenna design.

Table 1. Parameters of designed antenna.

Parameters	Value	Parameters	Value
l_1	7.25 mm	l_6	8.0 mm
l_2	2.5 mm	l_7	7.7 mm
l_3	16 mm	u_1	1.6 mm
l_4	6 mm	u_2	8.0 mm
l_5	18 mm	—	—

impedance are mainly dependent on the spiral and U-shaped loop lengths, respectively, and thus only a small number of iterations are needed.

B. Antenna Performance

The finally determined parameters of the designed antenna are summarized in Table 1. The simulated reflection coefficient of the antenna with the determined parameters in the skin tissue model, in which good resonance is achieved within the frequency band of 402 MHz to 405 MHz, is presented in Fig. 3. However, the resonant frequency increases to 478 MHz, and the matching deteriorates if the antenna is placed in air, as shown in Fig. 3. Moreover, the resonant characteristics of the designed antenna were analyzed in the cases of three different tissue types (skin, fat, and muscle), as shown in Fig. 3; the similar geometry was considered in [6]. As shown in Fig. 3, there is not a crucial shift in the resonant characteristics.

The radiated electromagnetic power from the implanted antenna is absorbed by the tissue surrounding the antenna, which gives rise to a critical issue related to patient safety. To preserve patient safety, the power incident on the implantable antenna should be limited to the maximum allowable level in accordance with maximum specific absorption rate (SAR), which is a generally accepted exposure measure. The IEEE C95.1 defined that the SAR averaged over any 1 g of cubic-shaped tissue be restricted to less than 1.6 W/kg ($SAR_{1\,g,\,max} \leq$ 1.6 W/kg) [23]–[24]. For this purpose, an SAR numerical analysis is performed at 403.5 MHz. Figure 5 shows the 1 g average SAR in decibels normalized to 321 W/kg (peak SAR value) when 1 W of power is delivered to the antenna. The simulation results indicate that the delivered power should be less than 4.99 mW to comply with the above-mentioned SAR restriction.

2. Parametric Studies

To understand the effects of the antenna parameters on antenna performance, parametric studies were carried out [25]. Four parameters; that is, spiral arm length, U-shaped loop

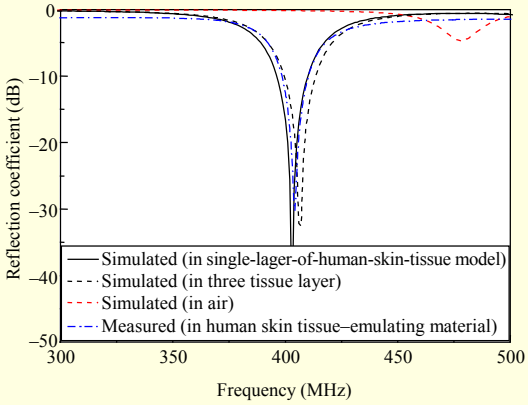

Fig. 3. Simulated and measured reflection coefficient of designed antenna.

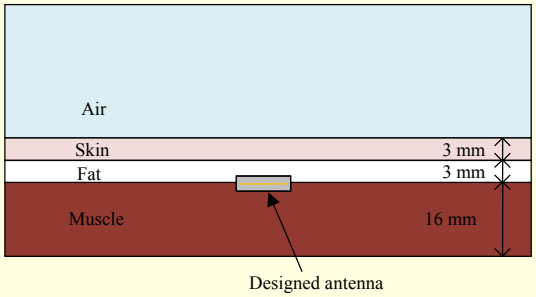

Fig. 4. Analysis model for antenna in three tissue layers.

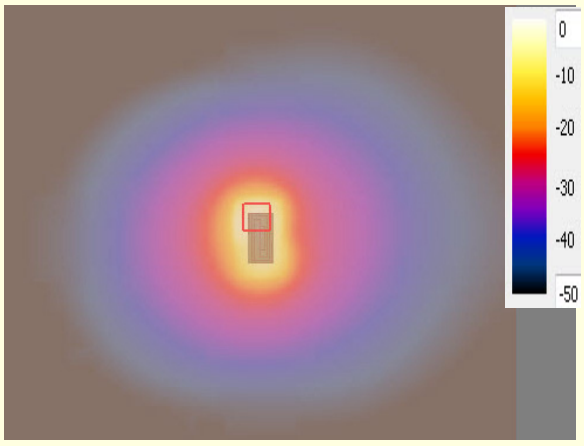

Fig. 5. Simulated 1 g average SAR distribution for designed antenna at a frequency of 403.5 MHz (normalized to 0 dB = 321 W/kg when the input power is 1 W).

length, material permittivity, and thickness, are considered in this study.

A. Effects of Spiral Arm Length

To evaluate the effects of the spiral arm length, the length of l_7, with the other parameters in Table 1 remaining unchanged,

ETRI Journal, Volume 37, Number 2, April 2015
http://dx.doi.org/10.4218/etrij.15.2314.0005

was changed and simulated in the same model shown in Fig. 2. The variations in reflection coefficient with respect to the spiral arm length (l_7) are presented in Fig. 6. As expected, a longer spiral arm length simultaneously increases the current path on the spiral patch and the effective size of the antenna, which results in a lowering of the resonant frequency.

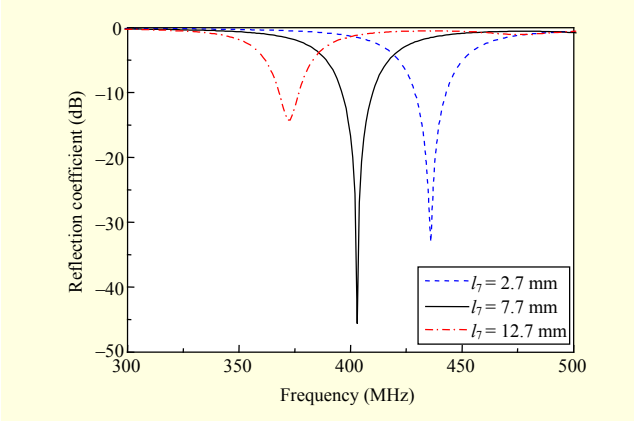

Fig. 6. Reflection coefficient with respect to spiral arm length (l_7).

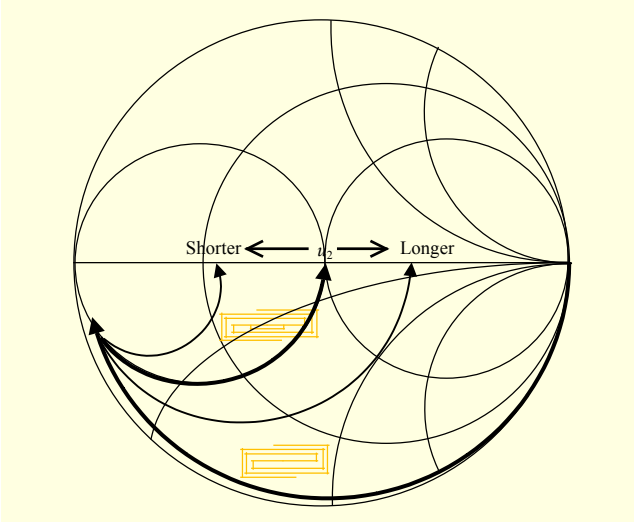

Fig. 7. Smith chart representing the impedance matching using a U-shaped loop.

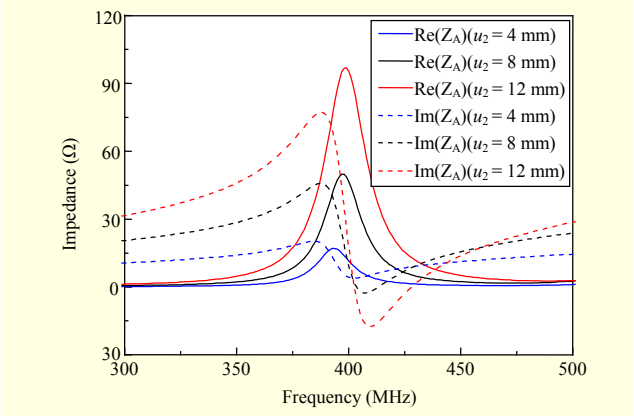

Fig. 8. Antenna impedance with respect to U-shaped loop length (u_2).

B. Effects of U-Shaped Loop Length

The proposed antenna has a U-shaped loop to make its impedance match that of the feeding circuit. The U-shaped loop gives a shunt inductance and cancels the capacitive reactance of the small spiral configuration; consequently, impedance matching is achieved. A conceptual description and the estimated impedance of the antenna impedance with respect to various u_2 (here, u_1 is fixed at 1.6 mm) are indicated in Figs. 7 and 8, respectively. As can be seen from these figures, keeping the resonant frequency fixed and increasing the value of u_2, we can observe that the real part of the impedance of the antenna increases while the imagery part remains at zero. Based on this study, the antenna impedance is adjusted by changing the length of u_2, and impedance matching can be attained.

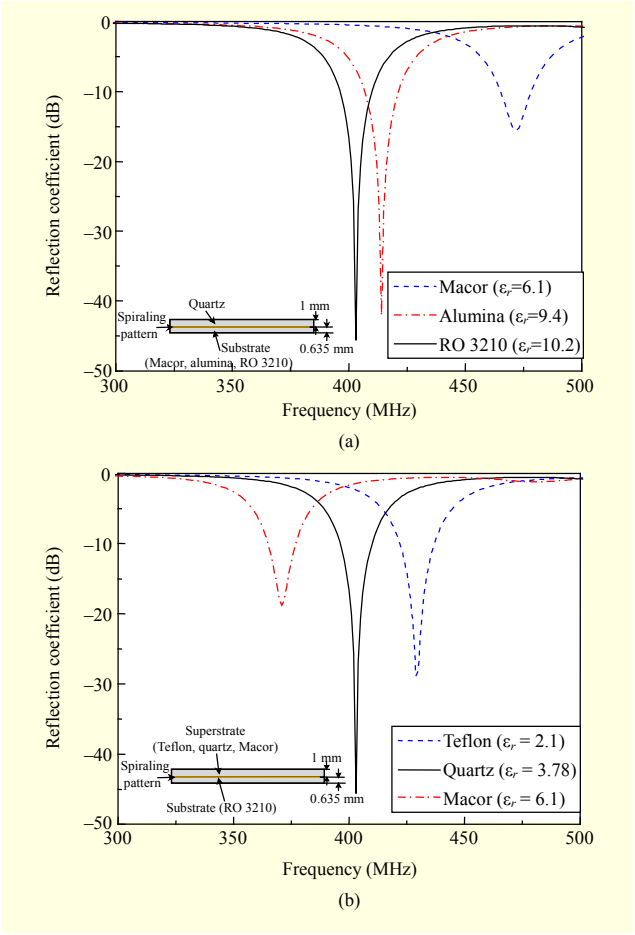

Fig. 9. Reflection coefficient with respect to (a) substrate and (b) superstrate materials.

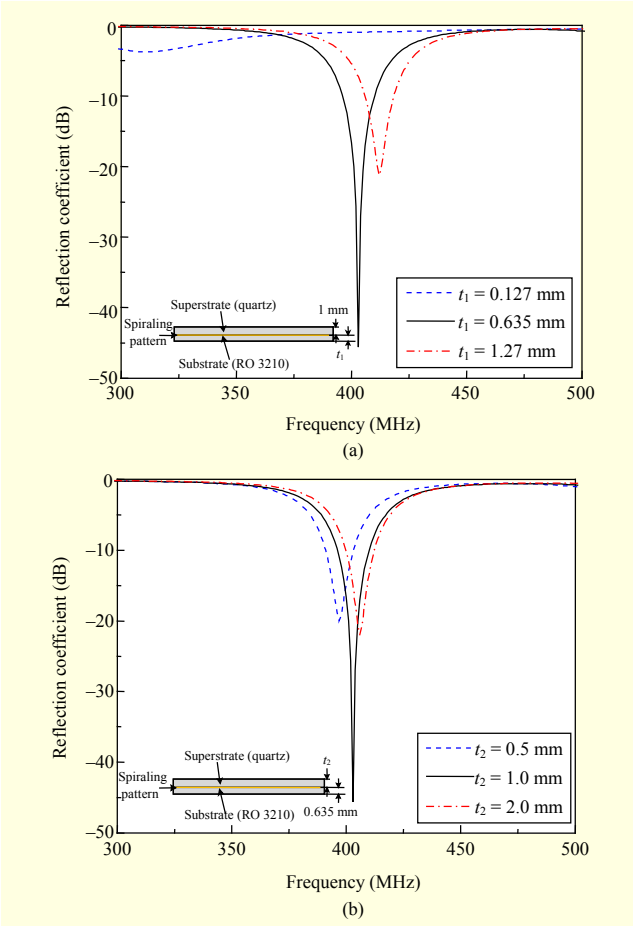

Fig. 10. Reflection coefficient with respect to (a) substrate and (b) superstrate thickness.

C. Effects of Substrate and Superstrate Materials

The selection of the substrate and superstrate materials is significant in the design of the antenna in terms of its long-term compatibility. Three commonly used substrate materials; that is, Macor, alumina, and RO 3210, all 0.635 mm in thickness, were compared, as shown in Fig. 9(a). In this comparison, quartz ($\varepsilon_r = 3.78$) was considered as the superstrate. The results reached our expectation; a higher permittivity of the substrate makes the effective wavelength shorter and the resonant frequency lower. The superstrate materials; that is, Teflon, quartz, and Macor, having the substrate of RO 3210 in common are also varied and a similar trend as with the substrate was obtained, as shown in Fig. 9(b). Therefore, a prudent choice of the substrate and superstrate materials is required to ensure the antenna performance.

D. Effects of Substrate and Superstrate Thickness

The effect of the material thickness on the antenna performance is also estimated. The substrate thickness (t_1) is changed with a fixed superstrate thickness (t_2) of 1 mm, and the superstrate thickness (t_2) is changed with a fixed substrate thickness (t_1) of 0.635 mm. As the materials thickness are increased, their respective effective permittivities decrease owing to the insulation of the antenna from the higher-permittivity tissue material; hence, the resonant frequency increases (see Fig. 10). However, for the extreme substrate thickness (t_1 = 0.127 mm) in Fig. 10(a), the impedance matching is degenerated, and the U-shaped loop should be adjusted for this thickness.

IV. Prototype Antenna, Tissue–Emulating Material Fabrication, and Measurement

1. Fabrication of Prototype Antenna and Tissue-Emulating Material

To verify the performance of the designed antenna, a prototype was fabricated, as shown in Fig. 11(a). A conducting spiral configuration and U-shaped loop structure of 18 μm in thickness were realized on a high-permittivity 0.635 mm thick Rogers RO 3210 ($\varepsilon_r = 10.2$, $\tan\delta = 0.03$) substrate and 1 mm thick quartz–glass (ε_r = 3.78) superstrate. For differential feeding, a balun (TDK ATB2012-50011) was soldered onto the bottom of the antenna, and an SMA connector was connected to the unbalanced line of the balun.

For the in-body operation environment of the antenna, gelatinous tissue–emulating material with similar electrical

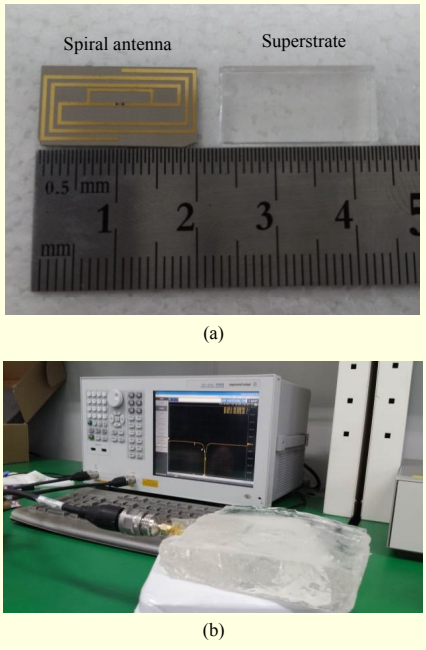

Fig. 11. Photographs: (a) fabricated antenna and (b) measurement setup for reflection coefficient.

ETRI Journal, Volume 37, Number 2, April 2015
http://dx.doi.org/10.4218/etrij.15.2314.0005

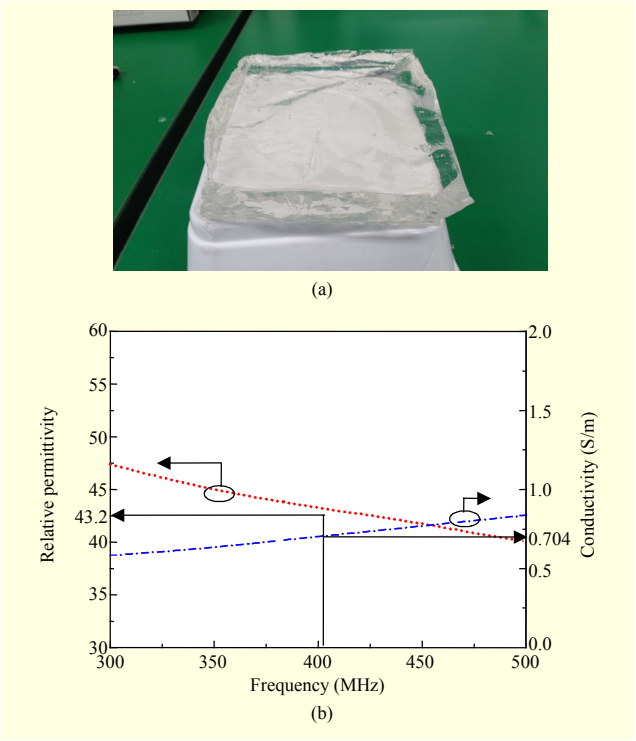

Fig. 12. Tissue–emulating material: (a) photo and (b) measured permittivity and conductivity.

properties as human skin in terms of permittivity and conductivity was also developed [26], as shown in Fig. 12(a). The tissue–emulating material is made of deionized water, sucrose, sodium chloride, and agarose. The recipes for the MICS band are given in Table 2. The development process can be briefly described as follows: i) sucrose and sodium chloride are melted in deionized water with slight warming, ii) agarose powder is added into the liquid solution and the mixture is stirred while heating until a clear solution forms, and iii) the mixture is cooled to room temperature. Here, agarose is used to solidify the liquid mixture for easy measurement. The permittivity and conductivity were measured using an Agilent 85070E dielectric probe kit and a network analyzer. Figure 12(b) shows the measured relative permittivity and conductivity of the gel; the values of which are 43.2 and 0.704 S/m at a frequency of 402 MHz, respectively. These measured values are acceptable within an allowable error of 10% in comparison with the desired values (ε_r = 46.7 and σ = 0.69 S/m at 402 MHz).

2. Measurement of Fabricated Antenna

The performance of the fabricated antenna was verified in terms of its resonance characteristics. The antenna was imbedded in the developed tissue–emulating gel, and the reflection coefficient was measured, as shown in Fig. 11(b).

Table 2. Recipes for human skin tissue–emulating material in the MICS band.

Ingredient	Mixing ratio
Sucrose	52.21%
Sodium chloride	2.79%
Deionized water	45%
Agarose	0.9 g / 100 ml solution

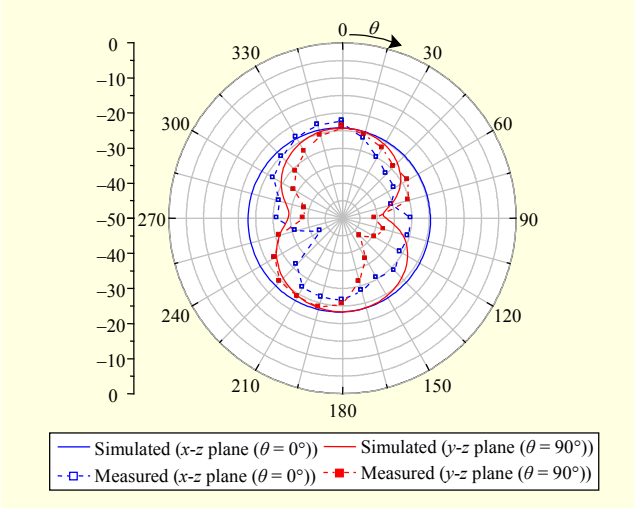

Fig. 13. Gain radiation pattern of designed antenna at 403.5 MHz.

The measured values are also shown in Fig. 3 for a comparison with the simulation results. The measured frequency band is within the range of 398 MHz to 410 MHz with a –10 dB bandwidth criterion (from 395 MHz to 409 MHz in the simulation). An antenna with a 1 mm longer spiral arm (l_7) and 1 mm shorter U-shaped loop (u_2) than the designed antenna shows good agreement with the simulation results, which is possibly due to the complex errors in the substrate permittivity, superstrate permittivity, thickness, tissue–emulating material, and manufacturing process.

The gain radiation patterns in the *x*-*z* and *y*-*z* planes at 403.5 MHz are measured and simulated, as shown in Fig. 13. Maximum gains of –22.26 dBi and –24.29 dBi are obtained from measurement and simulation, respectively. An antenna efficiency of 0.215% was obtained in measurement and is comparable to the antennas in [10], [14], [16], [20], and [22].

V. Conclusion

In this study, we considered an implantable rectangular spiral antenna for wireless biotelemetry in the MICS band (402 MHz to 405 MHz). In designing an implantable antenna, there

are requirements and constraints related to its small size, biocompatibility, impedance matching, far-field gain, and patient safety, among other factors. To miniaturize the antenna, a spiral configuration was adopted and realized on a high-permittivity substrate. The antenna impedance was adjusted using a U-shaped loop structure. The antenna impedance was easily adjusted by controlling the shape and length of the U-shaped loop. To preserve patient safety, a 1 g SAR distribution is estimated, and the incident power on the antenna should be less than 4.99 mW to comply with an SAR restriction of IEEE C95.1 ($SAR_{1\ g,\ max} \leq 1.6$ W/kg). Antenna parameters such as the spiral arm length; U-shaped loop length; and material and thickness of the substrate and superstrate were studied to understand their effect on the antenna performance. The potential of the designed antenna for biotelemetry application was demonstrated through a prototype fabrication and performance measurement based on the resonant characteristics and gain radiation pattern. A human skin tissue–emulating material was also developed to provide a real environment for the antenna. The measurements showed that the resonant characteristics were in good agreement with the simulations, and the frequency band ranged from 398 MHz to 410 MHz with a –10 dB bandwidth. A maximum gain of –22.26 dBi and an antenna efficiency of 0.215% were obtained.

References

[1] A.J. Johansson, "*Wireless Communication with Medical Implants: Antenna and Propagation*," Ph.D. dissertation, Dept. Elect. Eng., Lund Univ., Lund, Sweden, 2004.

[2] A. Rosen, M.A. Stuchly, and A.V. Vorst, "Application of RF/Microwave in Medicine," *IEEE Trans. Microw. Theory Techn.*, vol. 50, no. 3, Mar. 2002, pp. 963–974.

[3] W. Gao et al., "Transmission Power Control for IEEE 802.15.6 Body Area Networks," *ETRI J.*, vol. 36, no. 2, Apr. 2014, pp. 313–316.

[4] D. Panescu, "Emerging Technologies (Wireless Communication Systems for Implantable Medical Devices)," *IEEE Eng. Med. Biol. Mag.*, vol. 27, no. 2, Mar. 2008, pp. 96–101.

[5] K.S. Nikita et al., "Editorial: Special Issue on Mobile and Wireless Technologies for Healthcare Delivery," *IEEE Trans. Biomed. Eng.*, vol. 59, no. 11, Nov. 2012, pp. 3083–3089.

[6] J. Kim and Y. Rahmat-Samii, "Implanted Antennas Inside a Human Body: Simulations, Designs, and Characterizations," *IEEE Trans. Microw. Theory Techn.*, vol. 52, no. 8, Aug. 2004, pp. 1934–1943.

[7] *FCC*, *Medical Implant Communications*, 2003. Accessed Jan. 15, 2014. http://wireless.fcc.gov/services/index.htm?job=service_home &id=medical_implant

[8] W.G. Scanlon, N.E. Evans, and J.B Burns, "FDTD Analysis of Closed-Coupled 418 MHz Radiating Devices for Human Biotelemetry," *Physics Med. Biol.*, vol. 44, no. 2, Feb. 1999, pp. 335–345.

[9] G.C. Crumley et al., "On the Design and Assessment of a 2.45 GHz Radio Telecommand System for Remote Patient Monitoring," *Med. Eng. Physics*, vol. 20, no. 10, Feb. 1998, pp. 750–755.

[10] A. Kiourti and K.S. Nikita, "A Review of Implantable Patch Antennas for Biomedical Telemetry: Challenges and Solutions," *IEEE Antennas Propag. Mag.*, vol. 54, no. 3, June 2012, pp. 210–228.

[11] Z. Jin, J.-H. Lim, and T.-Y. Yun, "Small-Size and High-Isolation MIMO Antenna for WLAN," *ETRI J.*, vol. 34, no. 1, Feb. 2012, pp. 114–117.

[12] J.L. Volakis, C.-C. Chen, and K.Fujimoto, "*Small Antennas: Miniaturization Techniques & Applications*," New York, NY, USA: McGrawHill, 2010, pp. 131–208.

[13] A. Kiourti and K.S. Nikita, "Accelerated Design of Optimized Implantable Antenna for Medical Telemetry," *IEEE Antennas Wireless Propag. Lett.*, vol. 11, 2012, pp. 1655–1658.

[14] C.-M. Lee et al., "Compact Broadband Stacked Implantable Antenna for Biotelemetry with Medical Devices," *Electron. Lett.*, vol. 43, no. 12, June 2007, pp. 660–662.

[15] P. Soontornpipit, C.M. Furse, and Y.C. Chung, "Design of Implantable Microstrip Antenna for Communication with Medical Implants," *IEEE Trans. Microw. Theory Techn.*, vol. 52, no. 8, Aug. 2004, pp. 1944–1951.

[16] T. Karacolak et al., "In Vivo Verification of Implantable Antennas Using Rats as Model Animals," *IEEE Antennas Wireless Propag. Lett.*, vol. 9, 2010, pp. 334–337.

[17] W. Huang and A.A. Kishk, "Embedded Spiral Microstrip Implantable Antenna," *Int. J. Antennas Propag.*, 2011, pp. 1–6.

[18] S.I. Kwak, K. Chang, and Y.J. Yoon, "Small Spiral Antenna for Wideband Capsule Endoscope System," *Electron. Lett.*, vol. 42, no. 23, Nov. 2006, pp. 1328–1329.

[19] W. Huang and A.A. Kishk, "Embedded Spiral Microstrip Implantable Antenna," *Int. J. Antennas Propag.*, 2011, pp. 1–6.

[20] K.Y. Yazdandoost and R. Kohno, "Body Implanted Medical Device Communications," *IEICE Trans. Commun.*, vol. E92-B, no. 2, Feb. 2009, pp. 410–417.

[21] K. Sawasaki et al., "Design of Planar Antenna for Small Implantable Devices," *Proc. Int. Symp. Antennas Propag.*, Nagoya, Japan, Oct. 29–Nov. 2, 2012, pp. 1264–1267.

[22] A. Kiourti and K.S. Nikita, "Miniature Scalp-Implantable Antennas for Telemetry in the MICS and ISM Bands: Design, Safety Consideration and Link Budget Analysis," *IEEE Trans. Antennas Propag.*, vol. 60, no. 8, Aug. 2012, pp. 3568–3575.

[23] IEEE Std. C95.1-1999, *IEEE Standard for Safety Levels with Respect to Human Exposure to Radio Frequency Electromagnetic Fields, 3 kHz to 300 GHz*, IEEE, Piscataway, NJ,

USA, 1999.
[24] IEEE Std. C95.1-2005, *IEEE Standard for Safety Levels with Respect to Human Exposure to Radio Frequency Electromagnetic Fields, 3 kHz to 300 GHz*, IEEE, Piscataway, NJ, USA, 2005.
[25] A. Kiourti, M. Tsakalakis, and K.S. Nikita, "Parametric Study and Design of Implantable PIFAs for Wireless Biotelemetry," *Proc. ICST Int. Conf. Wireless Mobile Commun. Healthcare*, Kos Island, Greece, Oct. 5–7, 2011, pp. 96–102.
[26] T. Karacolak, A.Z. Hood, and E. Topsakal, "Design of a Dual-Band Implantable Antenna and Development of Skin Mimicking Gels for Continuous Glucose Monitoring," *IEEE Trans. Microw. Theory Techn.*, vol. 56, no. 4, Apr. 2008, pp. 1001–1008.

Jae-Ho Lee received his BS degree in electronic and electrical engineering from Kyungpook National University, Daegu, Rep. of Korea, in 2002 and his MS degree in electrical and electronic engineering from the Korea Advanced Institute of Science and Technology, Daejeon, Rep. of Korea, in 2004. He was awarded his PhD degree in electrical and electronic engineering from the Tokyo Institute of Technology, Japan, in 2010. From 2004 to 2005, he worked at the Mobile Communication PM team of the Institute of Information and Technology Assessment, Daejeon, Rep. of Korea. He also worked for the Radar Research Center at Samsung Thales, Yongin, Rep. of Korea, from 2010 to 2012. Since 2013, he has been a senior researcher with the Electronics and Telecommunications Research Institute, Daegu, Rep. of Korea. His research interests include waveguide arrays, electromagnetic numerical analysis, biomedical implantable devices, and antennas.

Dong-Wook Seo received his BS degree in electrical engineering from Kyungpook National University, Daegu, Rep. of Korea, in 2003 and his MS and PhD degrees in electrical engineering from the Korea Advanced Institute of Science and Technology, Daejeon, Rep. of Korea, in 2005 and 2011, respectively. He was a senior researcher at the Defense Agency for Technology and Quality, Daegu, Rep. of Korea, from 2011 to 2012. Since 2012, he has been a senior researcher with the Electronics and Telecommunications Research Institute, Daegu, Rep. of Korea. His current research interests include numerical techniques in the area of electromagnetics, radar cross-section analysis, wireless power transfer, and biomedical implantable devices.

Hyung Soo Lee received his BS degree in electrical engineering from Kyungpook National University, Daegu, Rep. of Korea, in 1980 and his PhD degree in IT Engineering from Sungkyunkwan University, Suwon, Rep. of Korea, in 1996. Since 1983, he has been a principal researcher with the Electronics and Telecommunications Research Institute, Daegu, Rep. of Korea. His research interests are spectrum engineering, WPAN system design, and biomedical IT convergence devices.